4

Coherent Effects in the Interaction of Laser Radiation with Tissues and Cell Flows

In this chapter, coherent effects that accompany the propagation of laser radiation in tissues and the interaction of laser radiation with cell flows are considered. These effects include diffraction, formation of speckle structures, interference of speckle fields, scattering from moving particles, etc. Principles of quasi-elastic light scattering (QELS) spectroscopy, diffusion wave spectroscopy (DWS), full-field speckle imaging (LASCA), confocal microscopy, optical coherence tomography (OCT), and second-harmonic generation (SHG) imaging are discussed.

4.1 Formation of speckle structures

Speckle structures are produced as a result of interference of a large number of elementary waves with random phases that arise when coherent light is reflected from a rough surface or when coherent light passes through a scattering medium.[45,76,77,82,83,112,113,129,136,139,155,157,343,396,821–837] The speckle phenomenon is a three-dimensional interference effect that exists in all points of space where the reflected or transmitted waves from an optically rough surface or volume intersect. Generally, there are two types of speckles: *subjective speckles*, which are produced in the image space of an optical system (including an eye), and *objective speckles*, which are formed in a free space and are usually observed on a screen placed at a certain distance from an object. Since the majority of bioobjects are optically nonuniform, irradiation of such objects with coherent light always gives rise to speckle structures that either distort the results of measurements and, consequently, should be eliminated in some way, or provide new information concerning the structure and the motion of a bioobject and its components. In this tutorial, we will mainly discuss the information aspects of speckle fields.

Figure 4.1 schematically illustrates the principles of the formation and propagation of speckles produced in the regime of transmission and reflection of coherent light in an optically nonuniform media; Fig. 4.2 shows a real speckle pattern formed at He:Ne laser beam transmission through a thin layer of a human epidermal sample. The average size of a speckle in the far-field zone is estimated as

$$d_{\mathrm{av}} \sim \lambda/\varphi, \tag{4.1}$$

where λ is the wavelength and φ is the angle of observation.

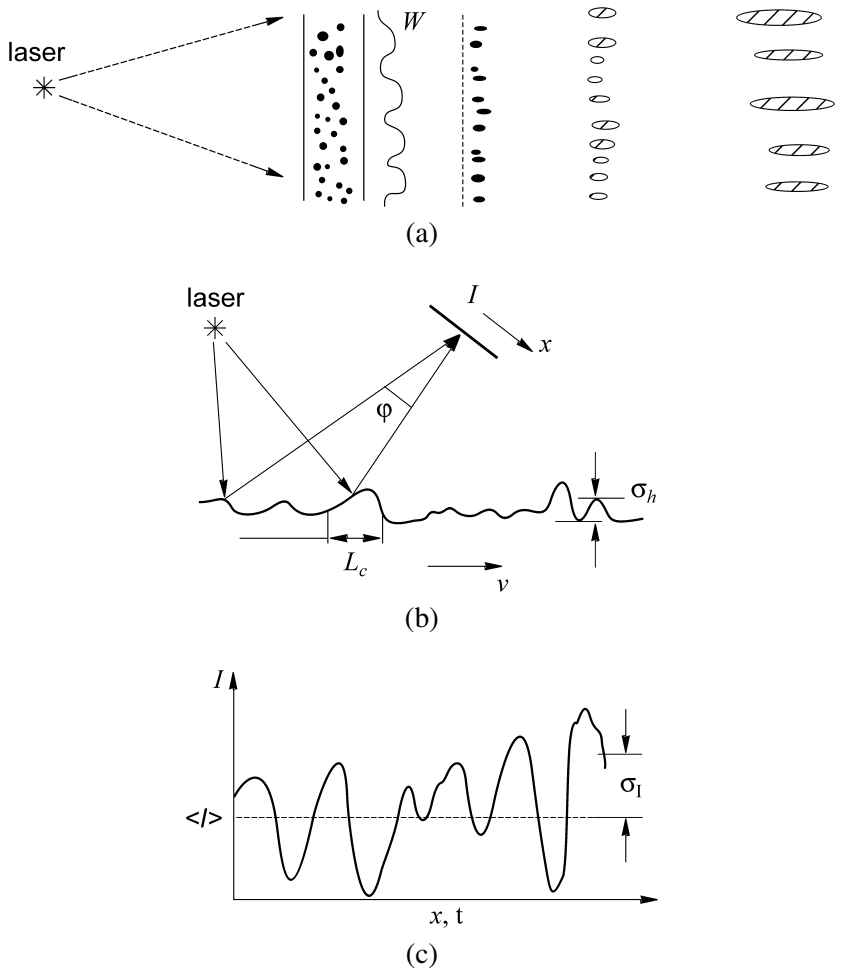

Figure 4.1 (a) Formation and propagation of speckles, (b) observation of speckles, and (c) intensity modulation; W is the scattered wave.[821]

Displacement x of the observation point over a screen or the scanning of a laser beam over an object with a certain velocity v (or an equivalent motion of the object itself with respect to the laser beam) when the observation point remains stationary gives rise to spatial or temporal fluctuations of the intensity of the scattered field. These fluctuations are characterized by the mean value of the intensity $\langle I \rangle$ and the standard deviation σ_I [see Fig. 4.1(b)]. The object itself is characterized by the standard deviation σ_h of the altitudes (depths) of inhomogeneities and the correlation length L_c of these inhomogeneities (random relief).

Since many tissues and cells are phase objects,[77,343] the propagation of coherent beams in bioobjects can be described within the framework of the model of a random phase screen (RPS).[75] The amplitude transmission coefficient of an RPS is given by

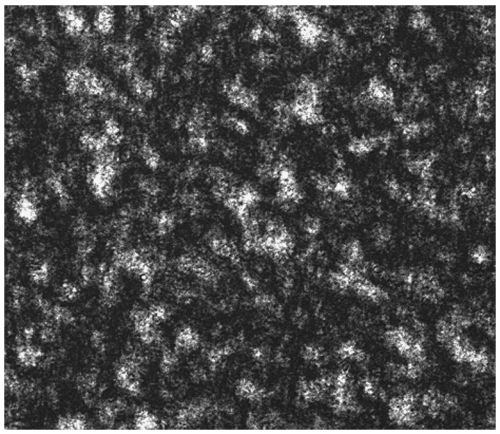

Figure 4.2 Speckle pattern produced at He:Ne laser beam transmission through a thin human skin epidermal sample (skin epidermal strip).

$$t_s(x, y) = t_0 \exp\{-i\,\Phi(x, y)\}, \tag{4.2}$$

where t_0 is the spatially independent amplitude transmission and $\Phi(x, y)$ is the random phase shift introduced by the RPS at the (x, y) point. Such spatial phase may be due to variations in the refractive index $n(x, y)$ or the RPS thickness $h(x, y)$ from point to point. For thin transmitting and reflecting RPSs, we have

$$\Phi(x, y) = \left(\frac{2\pi}{\lambda}\right)\{n(x, y) - 1\}h(x, y),$$

$$\Phi(x, y) = \left(\frac{4\pi}{\lambda}\right)h(x, y), \tag{4.3}$$

respectively. Phase fluctuations of the scattered field are characterized by the standard deviation σ_ϕ and the correlation length L_ϕ. Generally, there are two types of RPSs: weakly scattering RPSs ($\sigma_\phi^2 \ll 1$) and deep RPSs ($\sigma_\phi^2 \gg 1$).

The ideal conditions for the formation of speckles, when completely developed speckles arise, can be formulated in the following manner:

1. Coherent light irradiates a diffusive surface (or a transparency) characterized by Gaussian variations of optical length $\Delta L = \Delta(nh)$ with the probability density distribution

$$p(\Delta L) = \left\{2\pi\sigma_L^2\right\}^{1/2} \exp\left\{-\frac{(\Delta L)^2}{2\sigma_L^2}\right\}. \tag{4.4}$$

2. The standard deviation of relief variations is such that $\sigma_L \gg \lambda$; both the coherence length of light and sizes of the scattering area considerably exceed the differences in optical paths caused by the surface relief, and many scattering centers contribute to the resulting speckle pattern.

Statistical properties of speckles can be divided into statistics of the first and second orders. Statistics of the first order describe the properties of speckle fields at each point. Such a description usually employs the intensity probability density distribution function $p(I)$ and the contrast

$$V_I = \frac{\sigma_I}{\langle I \rangle}, \quad \sigma_I^2 = \langle I^2 \rangle - \langle I \rangle^2, \tag{4.5}$$

where $\langle I \rangle$ and σ_I^2 are the mean intensity and the variance of the intensity fluctuations, respectively. In certain cases, statistical moments of higher orders are employed. For example, in addition to contrast, generally defined as

$$V_I = \left(\frac{\mu_2}{\mu_1} \right)^{1/2}, \tag{4.6}$$

we can introduce the asymmetry parameter

$$Q_a = \frac{\mu_3}{\mu_2^{1.5}}, \tag{4.7}$$

which provides additional information concerning the scattering object. Here, the statistical moments are defined as

$$\mu_n = (N-1)^{-1} \sum_{j=1}^{N} (I_j - \mu_1)^n. \tag{4.8}$$

For ideal conditions, when the complex amplitude of scattered light has Gaussian statistics, the contrast is $V_I = 1$ (developed speckles), and the intensity probability distribution function (PDF) is represented by a negative exponential function as[157]

$$p(I) = \left(\frac{1}{\langle I \rangle} \right) \exp\left\{ -\frac{I}{\langle I \rangle} \right\}. \tag{4.9}$$

Thus, the most probable intensity value in the corresponding speckle pattern is equal to zero; i.e., destructive interference occurs with the highest probability.

Equation (4.9) is plotted as curve 1 in Fig. 4.3, and it can be seen that the most probable speckle is dark. The intensity PDF described by this equation can be produced only by the interference of light that is polarized all in the same manner,

resulting in a similarly polarized speckle pattern.[828] Thus, the scattering surface can not depolarize the scattered light. Materials into which the light does not penetrate and is scattered only a single time generally produce speckle patterns that have an intensity distribution in accordance with Eq. (4.9). On the other hand, materials into which the light penetrates and is subject to multiple scattering, such as most biological tissues, tend to depolarize the interfering light.

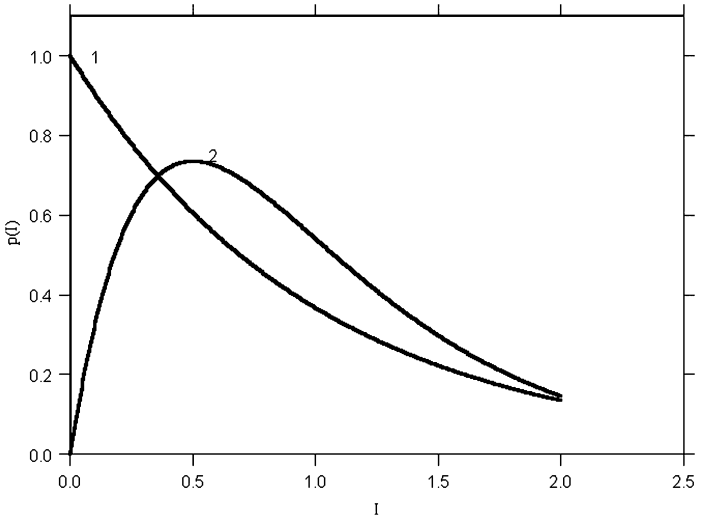

Figure 4.3 Theoretical intensity probability distribution functions $p(I)$ of a fully developed speckle pattern [curve 1, Eq. (4.9)] and the incoherent combination of two speckle fields [curve 2, Eq. (4.10)].[828]

Laser speckle patterns originating from most biological tissues are not "fully developed" in the sense that their intensity distribution does not follow a negative exponential relationship [Eq. (4.9)]. Such speckle patterns may have a distinctly different intensity PDF, one that is best thought of in terms of an incoherent combination of two speckle fields. Many speckle interferometers function by allowing two independent speckle patterns to interfere.[157,822–835] The speckle patterns can interfere either coherently or incoherently. In the case of a coherent combination, the statistical properties of the resulting third speckle pattern remain fundamentally the same as the two original patterns, typically following Eq. (4.9). However, in the case of an incoherent combination of two speckle fields, the final intensity PDF does not obey negative exponential statistics, but instead follows the equation[828]

$$p(I) = 4\left(\frac{I}{\langle I\rangle^2}\right)\exp\left\{\frac{-2I}{\langle I\rangle}\right\}. \tag{4.10}$$

The shape of this relationship is shown as curve 2 in Fig. 4.3. The intensity PDF of individual speckle patterns arising from most biological tissues obeys this equation. The reason is as follows: coherent light scattered from most biological tissues

produces randomly polarized speckle patterns, and any two orthogonally polarized components of scattered light are incoherent with one another. Thus, single speckle patterns arising from biological tissues that randomly polarize the speckle pattern can be considered to be the incoherent combination of two or more speckle patterns. Figure 4.4 shows the measured intensity PDF of a backscattered speckle pattern arising from illuminating a sample of porcine skin with an expanded He:Ne laser (633 nm). It is clearly seen that the intensity PDF of the scattered light from the skin more or less follows that predicted by Eq. (4.10).

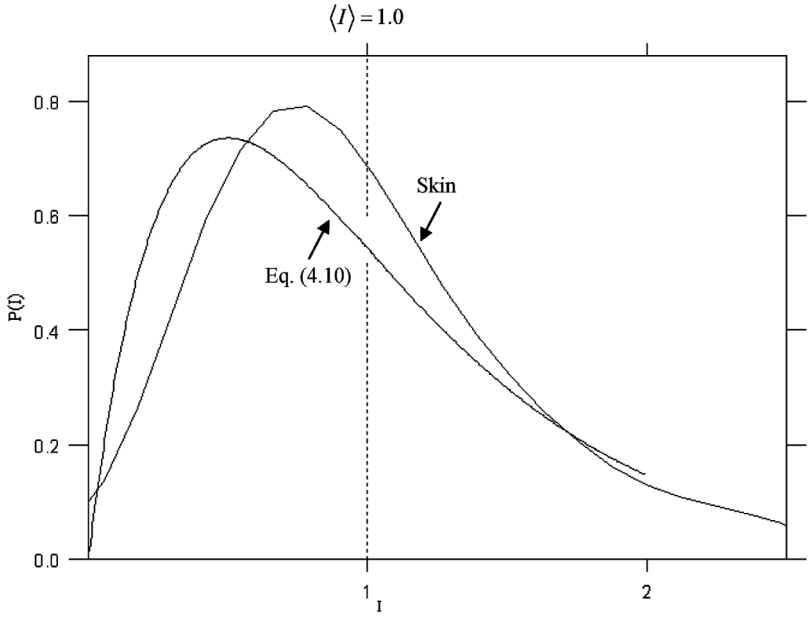

Figure 4.4 Measured intensity probability distribution function $p(I)$ of the speckle field generated by illuminating a sample of porcine skin with a He:Ne laser (633 nm) compared to that predicted by an incoherent combination of two fields [Eq. (4.10)].[828]

Partially developed speckle fields are characterized by a contrast $V_I < 1$. The contrast may be lower for the following reasons:

(1) If a uniform coherent background with intensity I_b is added to the speckle field, then we have

$$V_I = \left(1 - \rho_b^2\right)^{1/2}, \tag{4.11}$$

where $\rho_b = \langle I_b \rangle / (\langle I_b \rangle + \langle I \rangle)$. For example, with a decrease in the roughness of a surface (or the nonuniformity degree of a solid scatterer), we have $\sigma_\phi^2 \to 0$. Under these conditions, the strong specular (nonscattered) component of the coherent beam interferes with the speckle field. In the limiting

case of an ideally plane surface (a uniform medium), speckles vanish and $V_I = 0$.

(2) If a uniform incoherent background (e.g., due to lowering of the coherence of the light source or multiple scattering in the medium) arises, then we have

$$V_I = 1 - \rho_b. \tag{4.12}$$

For Gaussian statistics and a Gaussian correlation function of phase fluctuations, the propagation of intensity of the speckle field in a free space along the z-axis behind the RPS is described by the expression[75]

$$\sigma_I^2(z) = \left(\frac{\sigma_\phi^2}{2}\right)\left\{1 + \left(1 + D^2\right)^{-1}\right\}, \tag{4.13}$$

where $D = z\lambda/\pi L_\phi^2$ is the wave parameter. For a weakly scattering RPS ($\sigma_\phi^2 \ll 1$), the contrast of the speckle field is always less than unity. For a deep RPS ($\sigma_\phi^2 \gg 1$), the contrast reaches its maximum in the Fresnel zone ($D \cong 1$) when $z_{\max} = (2\pi/\lambda)(L_\phi^2/\sigma_\phi)$, $V > 1$. The fact that the contrast is higher than unity implies that dark areas predominate in the speckle pattern. The appearance of the maximum of intensity fluctuations is due to the focusing of scattered waves behind the RPS. In the Fraunhofer zone, we have $V_I \to 1$.

The intensity distribution for the light transmitted through an RPS can be represented in the following form:[75,157]

$$I_\Sigma(x, y) = I_c(x, y) + I_s(x, y). \tag{4.14}$$

Here, $I_c(x, y)$ is the intensity of light transmitted in the forward direction (the specular component) and $I_s(x, y)$ is the intensity of the scattered component. For a scattered field with Gaussian statistics, the intensity $I(0)$ at the center of the beam and the radius r_s of the scattered beam in the observation plane are determined by the following relations:

$$I(0) \cong I_0(0)\exp(-\sigma_\phi^2), \tag{4.15}$$

$$\begin{aligned} r_s &\cong \frac{z\lambda}{\pi L_\phi}, \quad \sigma_\phi^2 \ll 1, \\ r_s &\cong \left(\frac{z\lambda}{\pi L_\phi}\right)\sigma_\phi, \quad \sigma_\phi^2 \gg 1, \end{aligned} \tag{4.16}$$

where $I_0(0)$ is the intensity of the incident beam at its axis.

For both weakly scattering and deep RPSs moving with a velocity v in the direction perpendicular to the laser beam with a radius w, the correlation time of intensity fluctuations in the scattered field is given by[823]

$$\tau_c \cong \frac{2^{1/2} w}{v}. \tag{4.17}$$

This relationship holds true for a Gaussian incident beam when the observation plane lies in the Fraunhofer zone.

For phase objects with $\sigma_\phi^2 \gg 1$ and a small number of scatterers $N = w/L_\phi$ contributing to the field at a certain point in the observation plane, the contrast of the speckle pattern is greater than unity[824]

$$V_I = \left\{1 - \frac{2}{N} + \left(\frac{\sigma_\phi^2}{4N}\right) \exp\left[\left(\frac{2\pi L_\phi}{\lambda \sigma_\phi}\right) \sin\theta\right]^2\right\}^{1/2}, \tag{4.18}$$

where θ is the angle of observation (scattering angle). Note that the statistics of the speckle field in this case are non-Gaussian and nonuniform (i.e., the statistical parameters depend on the observation angle).

Statistics of the second order show how fast the intensity changes from point to point in the speckle pattern, i.e., they characterize the size and the distribution of speckle sizes in the pattern. The statistics of the second order are usually described in terms of the autocorrelation function of intensity fluctuations,

$$g_2(\Delta\xi) = \langle I(\xi + \Delta\xi) I(\xi) \rangle, \tag{4.19}$$

and its Fourier transform, representing the power spectrum of a random process; $\xi \equiv x$ or t is the spatial or temporal variable; $\Delta\xi$ is the change in variable. The angular brackets in Eq. (4.19) stand for the averaging over an ensemble or the time. To describe comparatively small intensity fluctuations, it is convenient to employ an autocorrelation function $\tilde{g}_2$ of the fluctuation intensity component and the corresponding structure function D_I,

$$\tilde{g}_2(\Delta\xi) = [\langle I(\xi + \Delta\xi) - \langle I \rangle \rangle][I(\xi) - \langle I \rangle], \tag{4.20}$$

$$\begin{aligned} D_I(\Delta\xi) &= \left\langle [I(\xi + \Delta\xi) - I(\xi)]^2 \right\rangle, \\ D_I(\Delta\xi) &= 2\left[\tilde{g}_2(0) - \tilde{g}_2(\Delta\xi)\right]. \end{aligned} \tag{4.21}$$

Analysis is usually performed in terms of normalized autocorrelation and structure functions. An autocorrelation function is preferable for the analysis of intensity

fluctuations caused by comparatively large inhomogeneities in the scattering object. At the same time, the structure function is more sensitive to small-scale intensity oscillations. Figures 4.5 and 4.6 display typical autocorrelation and structure functions measured for two types of normal and pathological tissues—epidermis of human skin and human tooth enamel.[77,343,834] These plots clearly illustrate the difference in the sensitivity of these functions to spatial fluctuations on different scales.

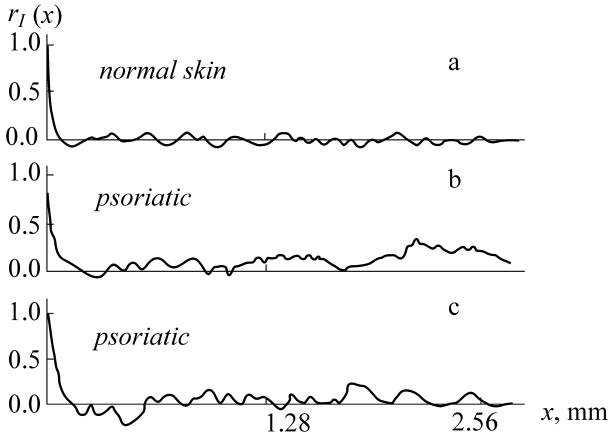

Figure 4.5 Normalized autocorrelation functions of intensity fluctuations in speckles $r_I(x)$ for thin layers of (a) normal and (b and c) psoriatic human epidermis probed with a focused laser beam.[77,343]

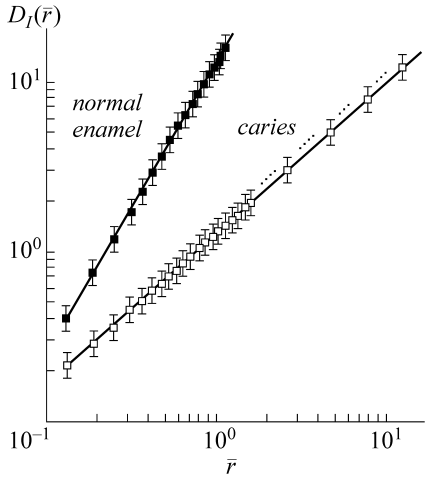

Figure 4.6 The difference between the structure functions of speckle fluctuations for the scattering of a focused laser beam from (the upper line) normal and (the lower line) pathological human tooth enamel (caries).[77,343]